

Published in final edited form as:

Neurobiol Aging. 2014 December ; 35(12): 2681–2690. doi:10.1016/j.neurobiolaging.2014.06.007.

Frontobasal gray matter loss is associated with the *TREM2* p.R47H variant

E.O. Luis, MSc^{1,#}, S. Ortega-Cubero, MD^{2,3,#}, I. Lamet, BSc³, C. Razquin, PhD², C. Cruchaga, PhD⁴, B.A. Benitez, MD⁴, E. Lorenzo, BSc², J. Irigoyen, BSN, MSc, RN^{2,3}, Alzheimer's Disease Neuroimaging Initiative (ADNI)[§], M.A. Pastor, MD, PhD^{1,3,5}, and P. Pastor, MD, PhD.^{*,2,3,5}

¹Neuroimaging Laboratory, Division of Neurosciences, Center for Applied Medical Research (CIMA), University of Navarra, Pamplona, Spain

²Neurogenetics Laboratory, Division of Neurosciences, Center for Applied Medical Research, University of Navarra, Pamplona, Spain

³Department of Neurology, Clínica Universidad de Navarra, University of Navarra School of Medicine, Pamplona, Spain

⁴Department of Psychiatry and Hope Center for Neurological Disorders, Washington University School of Medicine, St Louis, Missouri, United States of America

⁵CIBERNED, Centro de Investigación Biomédica en Red de Enfermedades Neurodegenerativas, Instituto de Salud Carlos III, Spain

Abstract

A rare heterozygous *TREM2* variant p.R47H (rs75932628) has been associated with an increased risk for Alzheimer disease (AD). We aimed to investigate the clinical presentation, neuropsychological profile and regional pattern of gray matter and white matter loss associated with the *TREM2* variant p.R47H, and to establish which regions best differentiate p.R47H carriers from noncarriers in two sample sets (Spanish and ADNI1). This was a cross-sectional study including a total number of 16 *TREM2* p.R47H carriers diagnosed with AD or mild cognitive impairment (MCI), 75 AD p.R47H noncarriers and 75 cognitively intact *TREM2* p.R47H noncarriers. Spanish AD *TREM2* p.R47H carriers showed apraxia (9 out of 9) and psychiatric symptoms such as personality changes, anxiety, paranoia or fears more frequently than in AD

© 2014 Elsevier Inc. All rights reserved.

*Correspondence and reprint requests: Dr. Pau Pastor, Neurogenetics Laboratory, Division of Neurosciences, Center for Applied Medical Research (CIMA), University of Navarra School of Medicine, Pfo XII 55, 31008-Pamplona, Spain. Tel.: +34 948194700; fax: +34 948194715. ppastor@unav.es.

#These authors contributed equally to this article.

§Some of the data used in preparation of this article were obtained from the Alzheimer's Disease Neuroimaging Initiative (ADNI) database (adni.loni.usc.edu). The investigators within the ADNI contributed to the design and implementation of ADNI and/or provided data but did not participate in analysis or writing of this report. A complete listing of ADNI investigators can be found at: <http://adni.loni.usc.edu>.

The authors report no conflicts of interest.

Publisher's Disclaimer: This is a PDF file of an unedited manuscript that has been accepted for publication. As a service to our customers we are providing this early version of the manuscript. The manuscript will undergo copyediting, typesetting, and review of the resulting proof before it is published in its final citable form. Please note that during the production process errors may be discovered which could affect the content, and all legal disclaimers that apply to the journal pertain.

noncarriers (corrected $p < 0.05$). For gray matter and white matter volumetric brain magnetic resonance imaging (MRI) voxel-wise analyses, we used statistical parametric mapping (SPM8) based on the General Linear Model. We used 3 different design matrices with a full factorial design. Voxel-based morphometry (VBM) analyses were performed separately in the two sample sets. The absence of inter-set statistical differences allowed us to perform joint and conjunction analyses. Independent VBM analysis of the Spanish set as well as conjunction and joint analyses revealed substantial gray matter loss in orbitofrontal cortex and anterior cingulate cortex with relative preservation of parietal lobes in AD/mild cognitive impairment (MCI) *TREM2* p.R47H carriers, suggesting that *TREM2* p.R47H variant is associated with certain clinical and neuroimaging AD features in addition to the increased *TREM2* p.R47H atrophy in temporal lobes described previously. The high frequency of pathological behavioural symptoms, combined with a preferential fronto-basal gray matter cortical loss, suggests that frontobasal and temporal regions could be more susceptible to the deleterious biological effects of the *TREM2* variant p.R47H.

1. INTRODUCTION

TREM2 (triggering receptor expressed on myeloid cells 2; OMIM: *605086) is a transmembrane glycoprotein which forms a receptor signaling complex with the TYRO protein tyrosine kinase binding protein. *TREM2* is mainly expressed in the microglia of the white matter, hippocampus, neocortex, cerebellum, basal ganglia, corpus callosum, medulla oblongata and spinal cord (R. Guerreiro, et al., 2013; Paloneva, et al., 2002). *TREM2* promotes the production of constitutive inflammatory cytokines in microglia (Bouchon, et al., 2000; Lanier and Bakker, 2000), leading to the phagocytosis of cell debris and amyloid (Paloneva, et al., 2002; Takahashi, et al., 2005). Recessive *TREM2* loss-of-function mutations cause Nasu-Hakola disease (NHD) or polycystic lipomembranous osteodysplasia with sclerosing leukoencephalopathy (PLOS; MIM 221770), which is characterized by early-onset frontal-like dementia and bone involvement (Hakola, 1972; Montalbetti, et al., 2005; Paloneva, et al., 2002). In addition, some families with inherited recessive fronto-temporal like dementia (FTD-like) with leukodystrophy without bone involvement carry *TREM2* mutations (R.J. Guerreiro, et al., 2013; Montalbetti, et al., 2005).

Recently, a rare *TREM2* variant (p.R47H; rs75932628-T) has been associated with susceptibility to late onset Alzheimer disease (AD) with an effect size similar to that of *APOE* $\epsilon 4$ (R. Guerreiro, et al., 2013; Jonsson, et al., 2013; Ruiz, et al., 2014). Although the role of p.R47H in protein function is not yet known, it has been proposed that this amino acid change at the immunoglobulin-like domain could impair the anti-inflammatory function of *TREM2* and facilitate amyloidogenic inflammatory response supported by its co-localization with amyloid plaques (Melchior, et al., 2010). Pathological examination of brains with *TREM2* rare variants including p.R47H revealed that all were in advanced AD (Braak stage 6) and most had typical findings with no distinguishing features except for the presence of mild Lewy-body and TAR DNA-binding protein 43 (TDP-43) disease in two of them (R.J. Guerreiro, et al., 2013). Interestingly, *TREM2* rare variants have also been inconsistently associated with other neurodegenerative diseases such as frontotemporal dementia (FTD) or Parkinson disease (Rayaprolu, et al., 2013; Ruiz, et al., 2014). These results suggest that *TREM2* dysfunction in AD brains can lead to more deleterious effects in

certain brain regions such as frontal lobes or basal ganglia than in subjects with AD not carrying *TREM2* damaging variants. However, no *TREM2* p.R47H-associated phenotypical clinical and neuropsychological features have been systematically described to date, in part due to the low frequency of the *TREM2* mutations (Reitz and Mayeux, 2013). In addition, *TREM2* expression studies across the human brain have demonstrated significant regional differences (Forabosco, et al., 2013), suggesting that certain cortical and subcortical brain regions could have an increased susceptibility owing to the mutant *TREM2* protein. In fact, a tensor-based morphometry study of the temporal lobe has recently reported 1.4–3.3% annual rates of increase of brain-volume loss in this area in *TREM2* p.R47H AD carriers compared with noncarriers (Rajagopalan, et al., 2013). However, no whole brain voxel-based morphometry (VBM) studies on *TREM2* variant carriers including gray and white matter are available.

Therefore, we aimed to investigate whether differences in clinical presentation and neuropsychological profile were associated with the *TREM2* variant p.R47H and to determine the regional pattern of gray matter and white matter loss associated with the *TREM2* p.R47H variant, to elucidate which regions best differentiate *TREM2* p.R47H carriers from AD/MCI noncarriers and from cognitively intact noncarriers p.R47H in two populations (Spanish and ADNI1). For that, we performed brain magnetic resonance imaging (MRI) VBM analysis separately in two sample sets (first the Spanish set and, secondly, the ADNI1 set in order to replicate the findings). After performing a full factorial two-way ANOVA that showed no specific intra-sample set morphometric differences, conjunction and joint analyses of both sets were also performed.

2. MATERIALS AND METHODS

2.1. Subjects

2.1.1. Genotyping of *TREM2* p.R47H variant and subject selection

Spanish set: Subjects with probable AD (n=550) and healthy controls (n=550) recruited at the Memory Disorders Unit, Department of Neurology, Clínica Universidad de Navarra, School of Medicine (Pamplona, Spain) were screened for *TREM2* p.R47H with a specifically designed KASPar assay as described (Benitez, et al., 2013). Early-onset AD (EOAD) subjects with relevant genetic AD variants were excluded by pooled-DNA next generation sequencing of exonic and flanking sequences in *APP*, *PSENI*, *PSEN2*, *MAPT* and *GRN* genes (Jin, et al., 2012). Prior to their participation, written informed consent was obtained from participant subjects or relatives.

ADNI1 set: The *TREM2* p.R47H variant was initially determined by direct genotyping (KASPar) in all the ADNI1 DNA as described (Benitez, et al., 2013). As whole-genome sequencing data had recently been released for the ADNI1 samples, we used these data to validate and confirm the genotype data. ADNI1 GWAS data (common variants Illumina 610) as well as HapMap data were used to calculate the principal component factors from population stratification using EIGENSOFT version 5.0.1 (Patterson, et al., 2006) to assure that all ADNI1 subjects had a European descent.

AD and MCI definition: All AD subjects (p.R47H carriers and non-carriers from both sets) fulfilled the NINCDS-ADRDA research criteria for probable AD (McKhann, et al., 1984). All AD patients from ADNI were in mild AD stages (MMSE scores between 20–26 and Clinical Dementia Rating (CDR) of 0.5–1). ADNI MCI subjects were defined as patients having memory complaints, low scores adjusted for education of Wechsler Memory Scale Logical Memory II b, MMSE scores between 24–30, CDR = 0.5, absence of significant impairment in other cognitive domains, absence of dementia and essentially preserved activities of daily living (adni.loni.usc.edu). MCI subjects from ADNI dataset were followed prospectively at 0, 6, 12, 18, 24 and 36 months, allowing to track the conversion from MCI to AD (Supplementary Table 6). When available, decreased levels of β -amyloid peptide 1–42 ($A\beta_{1-42}$) in cerebrospinal fluid (CSF) (< 192 pg/mL) were also considered as an AD predictor (Supplementary Table 6; Shaw, et al., 2009).

2.1.2. Subjects selected for the study

Spanish set: We found nine AD *TREM2* p.R47H heterozygous carriers, expanding our previously reported series (series details reflected in the Supplementary material) (Benitez, et al., 2013). In order to investigate whether *TREM2* p.R47H was associated with specific clinical and neuroimaging characteristics, nine AD *TREM2* p.R47H carriers (median age=69.3; range=57–84; 55.5% male) were compared with forty-eight AD p.R47H noncarriers (median age=70; range=52–83; 52% male) and forty-eight cognitively intact p.R47H noncarriers (median age=69.5; range=55–82; 48% male). These groups have similar gender proportion, age at onset (AAO), disease duration and age at evaluation to those of AD p.R47H carriers.

ADNI1 set: Neuroimaging and clinical data were obtained from *Alzheimer's Disease Neuroimaging Initiative* (ADNI1) database (adni.loni.usc.edu) subjects screened for presence of *TREM2* p.R47H (Supplementary material). Nine *TREM2* p.R47H carriers (median age=81; range=71–91; 55.5% male) were compared with 27 cognitively impaired *TREM2* p.R47H noncarriers (median age=78; range= 70–91; 55.5% male) and 27 cognitively intact p.R47H noncarriers (median age=79; range= 70–90; 55.5% male; Table 1). Seven *TREM2* p.R47H carriers and twenty *TREM2* p.R47H noncarriers belonged to the MCI research group (Supplementary Table 6). Among these MCI subjects, thirteen (4 carriers and 9 noncarriers) converted clinically to AD during follow-up, two MCI *TREM2* p.R47H noncarriers showed a MMSE decrease ≥ 5 points, five (1 carrier and 4 noncarriers) showed a CSF biomarker signature suggestive of AD ($A\beta_{1-42} < 192$ pg/mL) and the other seven (2 carriers and 5 noncarriers) remained cognitively stable during follow-up (Shaw, et al., 2009).

TREM2 p.R47H noncarriers with MCI, AD and cognitively intact, were selected with same gender proportion, age at onset (AAO), disease duration and age at evaluation to those of AD/MCI p.R47H carriers. All ADNI1 subjects selected for our study had European ancestry.

Review Board at the University of Navarra (Pamplona, Spain) and ADNI1 approved the study. Thus, considering both sets the total study sample was composed as follows: eighteen

AD/MCI p.R47H carriers, seventy-five AD/MCI p.R47H noncarriers and seventy-five cognitively intact p.R47H noncarriers (Table 1).

2.1.3. Clinical data and neuropsychological assessment

Spanish set: All AD subjects (p.R47H carriers and noncarriers) underwent a standard medical interview and a neurological examination by a neurologist specializing in cognitive disorders (M.A. Pastor, S. Ortega-Cubero and P. Pastor). Clinically relevant data, such as first-degree history of dementia or other neurological disorders, were recorded from their family relatives (Table 1). MRI scans were performed at the visit when diagnosis of MCI or AD was made. When the degree of cognitive decline was not severe (which was the situation with 62% of the sample), a complete neuropsychological examination was performed by a trained neuropsychologist (I. Lamet). The neuropsychological battery included the following tests: Mini Mental State Examination (MMSE) (Folstein, et al., 1975), long version of the Geriatric Depression Rating Scale (GDS) (Yesavage, et al., 1982), semantic verbal fluency (list of animals; Parkin and Java, 1999), Trail Making Test (TMT) parts A and B (Tombaugh, 2004), Alzheimer's disease assessment scale (ADAS) Word List (Mohs, et al., 1997) and 60-item Boston Naming Test (BNT; Williams, et al., 1989).

ADNI's set: Thirty-six MCI/AD ADNI1 subjects (p.R47H carriers and noncarriers) also underwent a cognitive assessment. Since the neuropsychological battery was not complete in all the subjects we selected the tests with more data available. Thus the tests selected were the following (the number of subjects who underwent this test is reflected in brackets): the clinical dementia rating sum of boxes (CDR-SOB) scale as a measure of cognitive and functional impairment (Morris, 1993; n=36), the MMSE (Folstein, et al., 1975) the ADAS Word list (Mohs, et al., 1997; n=36), GDS short form (Yesavage, et al., 1982; n=36), semantic verbal fluency (list of animals) (Parkin and Java, 1999; n=27), TMT-A and B (Tombaugh, 2004; n=27) and the 30-item BNT (Williams, et al., 1989; n=27). Two composite scores for memory and executive function (ADNI-MEM and ADNI-EF) were also recorded (Crane, et al., 2012; Gibbons, et al., 2012; n=34 and 33; respectively). More details about the neuropsychological assessment can be found on the ADNI website www.adni.loni.usc.edu.

2.2. Demographic, clinical and neuropsychological data analysis

The normality of the distribution and variance homogeneity of the numerical variables included in the study were tested using the Shapiro-Wilk and Levene's tests, respectively. ANOVA was applied to analyze differences between the means of these variables among the three study groups (AD/MCI *TREM2* p.R47H carriers, AD/MCI *TREM2* p.R47H noncarriers and healthy p.R47H *TREM2* noncarriers). A t-test was applied to search for differences between means when only the two AD/MCI study groups (AD/MCI *TREM2* p.R47H carriers and AD/MCI *TREM2* p.R47H noncarriers) were considered. Pure discrete counting variables were compared using the exact χ^2 -test.

All p-values were two-sided and all analyses were carried out using SPSS 15.0 software for Windows (SPSS Inc., Chicago, Illinois, USA) (Tables 1, 2 and 3).

Subsequently, neuropsychological data from both sets (Spanish and ADNI1) were analyzed to increase the statistical power. Both AD/MCI p.R47H carriers and AD/MCI p.R47H noncarriers subgroups were matched as following: each AD/MCI p.R47H carrier with three AD/MCI p.R47H noncarriers with similar gender, age at evaluation and age at onset to avoid a confounding effect of different distribution of neuropsychological variables between groups. After that, a conditional logistic regression model analyzing the relationship between neuropsychological variables and TREM2 p.R47H status, was individually applied for each neuropsychological test. The analysis was carried out using the program Epi InfoTM 7.1.2.0. Bonferroni correction was applied for multiple comparisons in all cases. The level of significance considered was $p < 0.05$ (Table 3).

2.3. Neuroimaging assessment

2.3.1. Data acquisition

Spanish set: Two of the 18 p.R47H carriers did not tolerate the 1.5 T MRI scan because of claustrophobia. Sixteen out of eighteen p.R47H carriers (ADNI1=9; Spanish=7), 74 cognitive impaired p.R47H noncarriers (ADNI1=27; Spanish= 47) and 74 cognitively intact p.R47H noncarriers (ADNI1=27; Spanish=47) underwent MRI scans. MRI studies of the Spanish subjects were all obtained on a 1.5-T Siemens Symphony scanner (Siemens, Erlangen, Germany). High-resolution volumetric images were acquired in a T1-weighted MR sequence in-plane resolution voxel size 1x1x1. **ADNI1 set:** The T1-weighted images from ADNI were obtained using three different 1.5 T scanners. Nine AD *TREM2* carriers, 12 AD *TREM2* noncarriers and 18 cognitively intact p.R47H noncarriers' images were acquired in a 1.5-T Siemens Symphony scanner. Ten of the remaining AD *TREM2* noncarriers and the healthy control images were acquired in a 1.5 TGE Medical Systems equipment. Finally, 5 AD/MCI *TREM2* noncarriers and 4 healthy control images were obtained with a Philips Medical Systems. Since the three image collections had different voxel sizes ($X_1=1.2$ mm; $Y_1=1.2$ mm; $Z_1=1.2$ mm; $X_2=0.92$ mm; $Y_2=0.92$ mm; $Z_2=0.92$ mm and $X_3=0.93$ mm; $Y_3=0.93$ mm; $Z_3=0.93$ mm), all T1-weighted images were resized to the sequence in-plane resolution voxel size 1x1x1 using *resize_img* function with Matlab.

2.3.2. MRI preprocessing—MRI images were processed with Statistical Parametric Mapping (SPM) software (SPM8; Wellcome Trust Centre for Neuroimaging; University College London, UK). For MRI VBM analysis, we used the VBM8 package (<http://dbm.neuro.uni-jena.de/vbm8/>). T1-weighted brain anatomical images were segmented using a unified segmentation procedure (Ashburner and Friston, 2005). For tissue segmentation a gray and white matter study-specific template (total of 164 volumes) was generated using the Diffeomorphic Anatomical Registration Through Exponentiated Lie Algebra algorithm (DARTEL) (Ashburner and Friston, 2005). This analysis concludes with the application of a spatial constraint to the segmented tissue probability maps, based on a Hidden Markov Random Field model (HMRF) (Cuadra, et al., 2005). We set 0.1 and 0.2 thresholds for gray matter and white matter, respectively. Subsequently, each image was spatially normalized into the standard space of the Montreal Neurological Institute template (MNI; Template-1_IXI550_mini152.nii). Image normalization included both linear components and non-linear transformations, which take into account individual regional differences in brain anatomy. A “Clean-up any partitions” procedure, particularly useful for atrophic

brains, was implemented using conditional dilations and erosions to better differentiate gray matter and white matter. We used “*Bias corrected image*” for quality control and also to create an average image of all normalized T1 images. Since spatial normalization expands or contracts some brain regions, modulation to gray matter and white matter was applied, scaling by the amount of contraction, to preserve the total amount of gray matter and white matter of the original images. The resulting gray matter and white matter images were modulated to correct individual brain size. Finally, images were smoothed with a Gaussian kernel (FWHM of 8 mm for gray matter).

2.3.3. Neuroimaging cross-sectional analysis—For gray matter and white matter volumetric voxel-wise analyses, we used statistical parametric mapping (SPM8) based on the General Linear Model. We used 4 different design matrices with a full factorial design: An ANOVA for the separate set analyses with the factor ‘subgroup’ with age and gender as nuisance variables; another ANOVA was performed to determine whether there were volumetric differences owed to any of the two clinical status (MCI and AD) in the ADNI1 set; a third ANOVA for analysing jointly the two sets with the factor ‘subgroup’ with age and gender as nuisance variables; and a two-way ANOVA for the analyses between sets with two factors “set” and ‘subgroup’ with age and gender as nuisance variables. The latter matrix was used for the conjunction analysis.

2.3.3.1. Separated gray matter volumetric analysis of Spanish and ADNI1 sets: Initially, we assessed gray matter volumetric differences between AD/MCI p.R47H carriers, AD/MCI p.R47H non-carriers and cognitively intact p.R47H noncarriers of the Spanish set. For this purpose, we conducted a full factorial analysis, an ANOVA with a factor ‘subgroup’ with 3 levels (AD/MCI p.R47H carriers, AD/MCI p.R47H non-carriers and cognitively intact p.R47H noncarriers). After determining a significant main effect of factor ‘subgroup’, pair-wise analyses were carried out by means of Statistical Parametric Mapping t-test (SPM-t) comparisons. The statistical threshold employed was $p < 0.05$ Family-Wise Error (FWE) cluster-wise corrected ($p = 0.001$ cluster-defining threshold, $t = 3.17$).

In a second step, we performed the same full factorial analysis for the ADNI1 set as followed for that of the Spanish sample. The contrasts analyzed were the following: AD/MCI p.R47H carriers vs. cognitively intact AD/MCI p.R47H noncarriers; AD/MCI p.R47H non carriers vs. cognitively intact AD/MCI p.R47H noncarriers and AD/MCI p.R47H carriers vs. AD/MCI p.R47H noncarriers. The same statistical threshold was employed for SPM-t comparisons $p < 0.05$ Family-Wise Error (FWE) cluster-wise corrected (cluster-defining threshold, $p = 0.001$, corresponding to $t = 3.24$ for the ADNI1 set).

2.3.3.1.1 Analysis of the presence of volumetric differences between AD and MCI subjects in ADNI1 set: In order to determine whether the clinical status of subjects (MCI and AD) could influence the results of ADNI1 set VBM analysis, we conducted a full factorial analysis for the ADNI1 set with factors: ‘group’, with 2 levels (AD/MCI p.R47H carriers and AD/MCI p.R47H non-carriers), ‘clinical status’, with 2 levels (AD and MCI), and their interaction ‘group x clinical status’.

2.3.3.2. Analysis of intra-sample set specific morphometric differences between

subgroups: In order to analyze jointly both sets we performed a new factorial analysis to determine homogeneity among subgroups: two-way ANOVA with a factor 'set' of two levels (Spanish and ADNI1 sets) and a factor 'group' with three levels (AD/MCI p.R47H carriers, AD/MCI p.R47H noncarriers and cognitively intact p.R47H noncarriers). Age at the time of the brain MRI scan and gender were considered as nuisance variables. To evaluate the presence of gray matter loss differences between the homologous subgroups from each set, the following SPM-t pair-wise analyses were carried out: AD/MCI p.R47H carriers from Spanish set vs. AD/MCI p.R47H carriers from ADNI1 set and AD/MCI p.R47H noncarriers from Spanish set vs. AD/MCI p.R47H noncarriers from ADNI1 set. This analysis showed no intra-sample set specific morphometric differences.

2.3.3.3 Conjunction analysis of Spanish and ADNI1 sets: We also performed a conjunction analysis with each subgroup of both sets to display statistically and topographically the maps of the common gray matter loss in both sets. For that, three new contrasts per dataset were generated: AD/MCI p.R47H carriers vs. AD/MCI p.R47H noncarriers, AD/MCI p.R47H carriers vs. cognitively intact p.R47H noncarriers and AD/MCI p.R47H noncarriers vs. cognitively intact p.R47H noncarriers. Each pair of t-contrasts (one for each dataset) was included in a separate conjunction analysis, following the method described by Friston (2005). Statistical significance was corrected for $p < 0.05$ FWE cluster-wise corrected (cluster-defining threshold, $p = 0.001$ and $t = 1.87$).

2.3.3.4 Joint analysis: Finally, a joint analysis of the two datasets was performed considering their homologous subgroups (AD/MCI p.R47H carriers, AD/MCI p.R47H noncarriers or cognitively intact p.R47H noncarriers), to obtain a higher statistical power. We performed a full factorial analysis: an ANOVA with the factor 'subgroup' of three levels (AD/MCI p.R47H carriers, AD/MCI p.R47H noncarriers and cognitively intact p.R47H noncarriers). Age at the time of the brain MRI scan and gender were considered as nuisance variables. After determining a significant mean effect of factor 'subgroup', the following pairwise SPM-t comparisons were carried out: AD/MCI p.R47H carriers vs. cognitively intact p.R47H noncarriers, AD/MCI p.R47H noncarriers vs. cognitively intact p.R47H noncarriers and AD/MCI p.R47H carriers vs. AD/MCI p.R47H noncarriers and AD/MCI p.R47H carriers vs. AD/MCI p.R47H noncarriers. Statistical significance was assessed with a FWE cluster-wise corrected p threshold < 0.05 (cluster-defining threshold, $p = 0.001$ and $t = 3.14$).

Leukoaraiosis, defined as the presence of hyperintense WM lesions in both T2-weighted and fluid attenuated inversion recovery (FLAIR) MRI sequences, was measured using the Scheltens semiquantitative visual rating scale (Scheltens, et al., 1993). Since basal ganglia calcifications were previously described in Nasu-Hakola patients (Klunemann, et al., 2005), the presence of brain calcifications was screened visually. We performed the same full factorial analysis to assess white matter volumetric changes as described for gray matter contrasts.

3. RESULTS

3.1. Clinical and neuropsychological findings

Spanish set: AD p.R47H carriers developed forgetfulness (7 out of 9) and depression (2 out of 9) as the main starting symptoms. During the first two years of the disease onset, minor depression and other psychiatric symptoms such as personality changes, anxiety, paranoia or fears appeared more frequently in AD p.R47H carriers compared with AD noncarriers ($p < 0.05$). Early spatial disorientation (8 out of 9) and apraxia (9 out of 9) were also reported often. Indeed, significant statistical differences were observed in the number of p.R47H carriers presenting with apraxia compared with noncarriers ($p < 0.05$; Table 2). Parkinsonian signs were more frequent in AD p.R47H carriers (66.7%) than AD p.R47H noncarriers (14.6%, $p < 0.05$). Other neurological symptoms less frequently observed among AD p.R47H carriers were somatic complaints (5 out of 9), sleep apnoea (3 out of 9), myoclonus (2 out of 9), seizures (1 out of 9), insomnia (1 out of 9), restless legs syndrome (1 out of 9) and somniloquism (1 out of 9). Clinical symptoms could not be evaluated in ADNI cohort since these data were not specifically recorded in ADNI1 subjects.

Both sets: Among 93 AD/MCI patients, MMSE scores were significantly lower in the p.R47H carriers group than in AD p.R47H noncarriers (mean 18 vs 21.6, $p < 0.05$; Table 1). However, the conditional logistic model showed no statistically significant association of any of the neuropsychological tests with the *TREM2* p.R47H status.

3.2. MRI findings

SWI-MRI sequences showed no brain calcifications or cerebral hemosiderin deposits in any p.R47H carrier. The degree of leukoaraiosis measured by the Scheltens scale showed similar scores between AD/MCI p.R47H carriers (mean=7.69; range:0–21) and AD/MCI noncarriers (mean=9; range:0–37; Table 1).

3.2.1. Independent VBM Analyses

3.2.1.1 Spanish set: The results of the ANOVA with a factor ‘subgroup’ with 3 levels (AD/MCI p.R47H carriers, AD/MCI p.R47H non-carriers and cognitively intact p.R47H noncarriers) showed a significant main effect of factor ‘subgroup’ ($F = 7.44$). Pair-wise Statistical Parametric Mapping t-test (SPM-t) between AD *TREM2* p.R47H carriers vs. cognitively intact p.R47H noncarriers showed gray matter loss among AD *TREM2* p.R47H carriers in bilateral middle orbitofrontal regions and left parietal lobe (angular and supramarginal gyri) and right hippocampus. Additionally, a lower volume in subcortical regions such as bilateral thalamus and putamen was observed among AD *TREM2* p.R47H carriers. Gray matter loss was also located in left middle temporal gyrus, inferior parietal regions and, bilaterally, in thalamic regions. For AD *TREM2* p.R47H carriers versus AD *TREM2* p.R47H non-carrier contrast, we found a lower gray matter volume in right orbitofrontal regions (Fig 1S and Supplementary material Table 1).

White matter VBM showed no significant differences in any of the three contrasts described above.

3.2.1.2. ADNI1 set: In order to replicate the findings of the VBM analysis of the Spanish sample, the ADNI1 set was also analyzed separately with an ANOVA following a similar design to the Spanish set. There was a significant main effect of factor ‘subgroup’ ($F=7.88$). Pair-wise analyses t-test (SPM-t) of ADNI1 AD/MCI *TREM2* p.R47H carriers vs. cognitively intact p.R47H noncarriers contrast not only showed a lower gray matter volume in rectal gyrus and temporal regions but also in subcortical regions including the right caudate nucleus, putamen and pallidum, amygdala and hippocampus. Other clusters with substantial gray matter loss were located bilaterally in middle and superior temporal gyri. The largest gray matter loss was observed in the right temporal pole. In addition, there was a significant gray matter volume decrease in middle frontal and cingulate gyri, superior and inferior parietal cortex and precuneus. At subcortical level, putamen and cerebellar vermis were the most affected regions. Finally, in the AD/MCI *TREM2* p.R47H carriers vs. AD/MCI *TREM2* p.R47H non-carriers contrast, a nonsignificant gray matter loss in bilateral orbitofrontal regions was observed. (Fig 1S and Supplementary material Table 2).

For white matter volumetric analysis, as observed in the Spanish set analysis, we found no statistically significant differences between subgroups across the ADNI1 set.

3.2.1.2.1 Analysis of the presence of volumetric differences between AD and MCI subjects in ADNI1 set: Since we found no differences in the comparison of AD/MCI *TREM2* p.R47H carriers vs. AD/MCI *TREM2* p.R47H non-carriers of the ADNI1 set, we conducted an additional analysis to assess the influence of diagnostic groups (MCI and AD) on the results. None of the factors (group, clinical status or the interaction) were significant ($F=13.89$; data not shown) suggesting that cerebral grey matter loss was similar in MCI and AD subjects. Thus, we concluded that the inclusion of MCI subjects along with AD subjects in the analysis would not change the results of the ADNI1 contrast.

3.2.2. Analysis of intra-sample set specific morphometric differences between subgroups

3.2.2.1. Factorial analysis between Spanish and ADNI1 sets: Regarding the factorial analysis using a two-way ANOVA to determine the homogeneity of the datasets, the main effect of the factor “set” revealed no statistical significance ($F=7.24$) but the subgroup factor, as expected, was significant ($F=11.60$). Interaction of the factor “set” / factor “subgroup” was not statistically significant. Pairwise t-test contrasts comparing homologous subgroups between sets: AD *TREM2* p.R47H carriers ADNI1 set vs. AD *TREM2* p.R47H carriers Spanish set and AD *TREM2* p.R47H noncarriers ADNI1 set vs. AD *TREM2* p.R47H noncarriers Spanish set were not significant. These results suggested that there were low chances of finding differences resulting from comparisons between AD/MCI *TREM2* p.R47H carriers, AD/MCI *TREM2* p.R47H noncarriers and cognitively intact p.R47H noncarriers due to a set effect (Spanish vs. ADNI1).

3.2.2.2. Conjunction analysis of Spanish and ADNI1 sets: A conjunction analysis of Spanish and ADNI1 sets was performed using the aforementioned factorial analysis. We observed significant common areas of gray matter loss among the homologous pairs of subgroups of each set. When compared with cognitively intact p.R47H noncarriers, the

AD/MCI p.R47H carriers (Spanish vs. ADNI1 sets) showed common gray matter loss in superior and inferior frontal regions, mesial temporal areas including amygdala, hippocampus and superior and inferior parietal areas. Regarding subcortical structures, we found common decrease of the gray matter in thalamus, cerebellum and basal ganglia, specifically in putamen and pallidum (Supplementary material Table 3, Figure 2A).

AD/MCI p.R47H noncarriers vs. cognitively intact p.R47H noncarriers (Spanish vs ADNI1 sets) showed common gray matter loss in hippocampus and amygdala together with frontal and parietal areas. At subcortical level common loss of gray matter volume was located in thalamus and cerebellum. (Supplementary material Table 3, Figure 2BS).

Finally, the common gray matter loss region in both sets (Spanish and ADNI1) resulting from the contrast of AD *TREM2* R47H carriers vs. AD *TREM2* R47H noncarriers was located in the orbitofrontal gyrus and anterior cingulate gyrus (Supplementary material Table 3, Figure 2C).

3.2.3. Joint analysis

3.2.3.1. Gray matter VBM analysis: The ANOVA of the two sets joined showed a significant main effect of 'subgroup' ($F = 7.22$).

Comparison between AD/MCI *TREM2* p.R47H carriers vs. cognitively intact p.R47H noncarriers: The 16 AD/MCI p.R47H carriers compared with 74 cognitively intact p.R47H noncarriers showed severe gray matter volume loss ($p < 0.05$ FWE cluster-wise corrected) in the following regions: bilateral rectal *gyri* (orbitofrontal cortex), bilateral middle temporal and amygdala. The maximum gray matter volume loss was observed in right rectal gyrus (t values of 10.28). Interestingly, parietal lobes were relatively spared in AD/MCI p.R47H carriers. With regard to the basal ganglia, gray matter loss was observed in both putamen and caudate nuclei among p.R47H carriers. The thalamic atrophic clusters showing greater degree atrophy were located in the ventral lateral nucleus, a relay nucleus with connectivity to the sensorimotor cortex (Figure 1A and Supplementary material Table 4).

Comparison between AD/MCI *TREM2* noncarriers vs. cognitively intact p.R47H noncarriers: We observed widespread gray matter loss in the 74 AD/MCI *TREM2* noncarriers compared with 74 cognitively intact p.R47H noncarriers ($p < 0.05$ FWE cluster-wise corrected) with a predominant distribution in temporal and parietal lobes compared to frontal lobes. The temporal atrophic areas were located bilaterally in middle temporal gyrus, where the maximum gray matter loss was found (t value = 15.56), as well as in mesial temporal areas including the hippocampus and amygdala. The hippocampal gray matter loss was more pronounced in the left side. This pattern was consistent with the results of previous VBM studies performed in AD-control series.²⁵ The second maximum region with gray matter loss outside the temporal lobes was located in the angular *gyrus* extending to the supramarginal *gyrus* predominantly on the left (t values of 15.14 and 14.94, respectively). Regarding subcortical structures, we found atrophy in ventral lateral thalamic nuclei (Figure 1B and Supplementary material Table 5).

Comparison between AD/MCI *TREM2* p.R47H carriers vs. AD/MCI *TREM2* p.R47H noncarriers: We performed a direct comparison between 16 AD/MCI p.R47H carriers and 74 cognitively intact p.R47H noncarriers. In this comparison, we identified significant gray matter loss in bilateral anterior cingulate cortex, left superior medial gyrus and bilateral rostro-ventral putamen, caudate heads and accumbens nuclei (Table 4 and Figure 1C). These results suggest that the presence of *TREM2* p.R47H could be associated with a gray matter loss pattern with impairment of prefrontal and frontobasal regions with relative preservation of parietal lobes.

3.2.3.2 White matter VBM analysis: The same contrasts were performed to compare using voxel based morphometry white matter brain volumes though no statistically significant differences were found among the groups.

4. DISCUSSION

In this study we investigate whether the novel *TREM2* p.R47H variant is associated with particular phenotypical (clinical and neuroimaging) features compared with cognitively impaired and healthy subjects who were p.R47H non carriers, as described for other genetic markers (Cruchaga, et al., 2009; Goni, et al., 2013). One important consideration is that the sets analyzed in our study were different with regard to recruitment methods: The Spanish set is a clinical cohort-based case-control sample whereas the ADNI1 is a longitudinal cohort with three different cognitive statuses (AD, MCI and healthy controls). Thus, differences in the recruitment and in the clinical data collection made it difficult to fully compare certain clinical and neuropsychological variables.

With regard to the clinical characteristics of the Spanish set, most of the AD p.R47H carriers presented an initial amnesic syndrome, as observed for AD p.R47H noncarriers. However, AD p.R47H carriers showed depression and personality changes at early stages evolving rapidly into multi-domain dementia. Visuospatial disorientation and parkinsonism appeared early in the majority of AD p.R47H carriers. Indeed, the p.R47H variant has been also associated with Parkinson's disease (Benitez and Cruchaga, 2013; Rayaprolu, et al., 2013), though these findings need further replication.

We found that the p.R47H carriers showed, especially in the Spanish sample, a multidomain severe cognitive progression associated with p.R47H and poor performance in MMSE (MMSE was 10 in 5 p.R47H AD carriers), suggesting that the p.R47H variant could lead in some cases to a more aggressive dementia. This impression is also supported by the increased temporal lobe atrophy found in a 24-month recent follow-up study among *TREM2* p.R47H mutation carriers (Rajagopalan, et al., 2013). Although MMSE showed lower scores among AD/MCI *TREM2* p.R47H carriers compared with noncarriers (mean MMSE scores 18 and 21.6, respectively), the conditional logistic regression analysis showed no influence of p.R47H in any of the neuropsychological tests analyzed, suggesting that more studies are necessary to demonstrate that the *TREM2* variants can lead to a more aggressive AD phenotype.

The *TREM2* p.R47H AD phenotype observed in the Spanish series has some similarities to the NHD phenotype (R.J. Guerreiro, et al., 2013). Subjects with NHD usually appear to show a frontal-like syndrome, but asymptomatic NHD p.Q33X *TREM2* heterozygous carriers can display subclinical impairment of short and long term visuo-spatial memory as observed in our AD p.R47H series (Montalbetti, et al., 2005). These results suggest that medial structures can be early impaired by loss-of-function *TREM2* heterozygous variants. On the other hand, few healthy p.R47H carriers have also been reported, indicating that p.R47H can behave as an AD risk variant with a large effect size but with incomplete penetrance (Jonsson, et al., 2013). Indeed, only ten out of eighteen p.R47H carriers had first-degree relatives with dementia. However, family segregation analysis and with longer follow-up studies of *TREM2* p.R47H carriers will help in clarifying this point.

Voxel-based morphometry (VBM) analyses were performed separately in the two sample sets. The analysis of the Spanish set showed a gray matter loss in the AD *TREM2* p.R47H carriers compared with cognitively intact p.R47H noncarriers in bilateral middle orbitofrontal regions and left parietal lobe (angular and supramarginal gyri), right hippocampus and in subcortical regions such as thalamus and putamen (Fig 1S and Supplementary material Table 1). In AD *TREM2* p.R47H carriers versus AD *TREM2* p.R47H non-carriers contrast, we found a lower gray matter volume in right orbitofrontal regions (Fig 1S and Supplementary material Table 1). In order to replicate the VBM analysis findings of the Spanish sample, we performed an independent analysis with the ADNI1 set. We found similar location of gray matter loss resulting from the comparison of AD/MCI *TREM2* p.R47H carriers vs. cognitively intact p.R47H noncarriers in rectal gyrus, middle frontal and cingulate gyri, superior and inferior parietal cortex and precuneus temporal regions, amygdala, hippocampus and in subcortical regions including the right caudate nucleus, putamen and pallidum. The AD *TREM2* p.R47H carriers vs. AD *TREM2* p.R47H non-carriers contrast, showed gray matter loss in bilateral orbitofrontal regions but it did not survive the level of significance (Fig 1S and Supplementary material Table 2). The lack of replication of the results of the Spanish sample in the ADNI1 sample could be due to several reasons. The Spanish subjects were in more advanced AD stages (mean MMSE 12.7) and had a longer disease duration than the ADNI1 MCI/AD subjects (mean MMSE 23.3) since in the ADNI1 dataset only subjects with mild AD were included. This observation suggests that *TREM2* p.R47H carriers could develop higher atrophy over time rates than noncarriers as supported by Rajagopalan and colleagues (Rajagopalan, et al., 2013) and thus increase differences in later disease stages. Another explanation for the lack of replication might be that the inclusion of MCI subjects could have diluted the results, but the lack of volumetric differences between MCI and AD subjects of ADNI1 suggested that most MCIs from ADNI1 were at pre-clinical AD stages.

In order to increase the sample, we confirmed the absence of intra-set statistical differences which allowed us to perform joint and conjunction analyses. Conjunction and joint analyses revealed substantial gray matter loss in orbitofrontal cortex and anterior cingulate cortex with relative preservation of parietal lobes in AD/MCI *TREM2* p.R47H carriers.

Thus, considering the analyses globally, the pattern of gray matter loss we observed in AD/MCI p.R47H carriers compared with healthy controls displayed some similarities and

differences with regard to the typical gray matter loss pattern described for AD (Goni, et al., 2013; Ishii, et al., 2005). The largest atrophic clusters were located bilaterally in both hippocampal regions and the ventromedial prefrontal cortex followed by the anterior cingulate cortex, extending to the basal forebrain and putamen. The VBM direct comparison between of AD/MCI p.R47H carriers with AD/MCI *TREM2* p.R47H noncarriers showed significant bilateral gray matter loss in the ventromedial prefrontal cortex, including the orbitofrontal cortex, rostral anterior cingulate cortex, ventral striatum and basal forebrain. The orbitofrontal clusters with gray matter loss correspond in the macaque brain to both the *orbital network*, involved in sensory integration and reward; and to the *medial network*, which modulates the visceral activity in response to affective stimuli (Hikosaka and Watanabe, 2000; Ongur, et al., 2003; Ongur and Price, 2000). Interestingly, the most extensive connections of the orbitofrontal cortex are set with the mesial temporal lobe, including hippocampal field CA1, entorhinal and perirhinal cortices and amygdala, indicating critical role of orbitofrontal cortex in integrative memory that links purpose and personal experience with contextual cues in order to produce judicious behavior (Cavada, et al., 2000). In humans, the orbitofrontal cortex shows a richer functional parcellation with subdivisions connected to association cortical areas such as prefrontal cortex, medial frontal limbic areas including anterior cingulate cortex and striatum (Kahnt, et al., 2012). The impairment of regions involved in emotional control and the integration of multimodal sensory information as well as the impairment of the anterior cingulate cortex regions (Bush, et al., 2000) could explain the early presentation of psychiatric symptoms, personality changes and visuospatial disorientation observed in AD/MCI p.R47H carriers (Table 4; Fig 1C). Interestingly, the frontal gray matter loss pattern observed in *TREM2* p.R47H carriers could explain the possible association of certain *TREM2* rare variants with clinical FTD (Lattante, et al., 2013; Rayaprolu, et al., 2013; Ruiz, et al., 2014).

Although the putaminal atrophy was present in both carriers and non carriers (see conjunction analysis comparing AD/MCI p.R47H noncarriers with cognitively intact AD/MCI p.R47H noncarriers, Figure 1), the differential volume loss in AD/MCI p.R47H carriers included accumbens and nucleus basalis of Meynert area in addition to the rostro-ventral putamen and caudate heads. The decreased putamen gray matter loss volume observed has been also described in some familial AD series (Cash, et al., 2013; Ryan, et al., 2013). The areas of the ventral striatum are connected with the orbito frontal cortex and anterior cingulate and receive dopaminergic input from the midbrain. In addition, such areas have a key role in reward processing. We hypothesize that degeneration of these *nuclei* could be related to the parkinsonian signs seen among some Spanish AD p.R47H carriers. Unfortunately, the lack of detailed clinical information in the ADNI1 series did not allow us to confirm these findings.

Leukoaraiosis is a common feature of NHD caused by *TREM2* recessive mutations (Paloneva, et al., 2002). However, there were neither significant differences between the two AD/MCI groups in Sheltens scale (Table 1) nor clusters with white matter volume loss among *TREM2* p.R47H carriers, suggesting that larger AD *TREM2* series are needed to further evaluate the white matter subcortical impairment caused by the p.R47H variant. However, although the density of microglia in the normal human brain is greater in white

matter than in gray matter (Mittelbronn, et al., 2001), it is possible that among the p.R47H carriers AD brain, the impaired microglia function to prevent amyloid accumulation and clear cellular debris may produce changes in the microglia mainly at cortical level with relative preservation of white matter glia.

In summary, our results suggest that frontobasal cortical regions could be more susceptible to the deleterious biological effects of the *TREM2* p.R47H variant. We are aware that our results are preliminary, based on a limited sample size with no follow-up, which suggests that we have to interpret these results cautiously and wait for them to be confirmed in larger AD series.

Supplementary Material

Refer to Web version on PubMed Central for supplementary material.

Acknowledgments

We thank all participating subjects and their relatives for their contribution to the study. We thank Drs Francisco Guillen-Grima and Marta Vidorreta for their statistical assessment. This work was supported by grants to P. Pastor from the Department of Health of the Government of Navarra, Spain (refs.13085 and 3/2008) and from the UTE project FIMA, Spain to P.P; E.O.L., is supported by an Education Department grant from Government of Navarra (2011–2014). C. Razquin holds a “Torres Quevedo” fellowship from the Spanish Ministry of Science and Technology, co-financed by the European Social Fund. Genotyping for the R47H variant in the Spanish and ADNI samples was supported by NIH grants (R01-AG044546 and P30-NS069329), the Alzheimer Association (NIRG-11-200110) and the American Federation for Aging Research (CC).

Data collection and sharing for this project was funded by the Alzheimer’s Disease Neuroimaging Initiative (ADNI) (National Institutes of Health Grant U01 Ag024904). ADNI is funded by the National Institute on Aging, the National Institute of Biomedical Imaging and Bioengineering, and through generous contributions from the following: Alzheimer’s Association; Alzheimer’s Drug Discovery Foundation; BioClinica, Inc.; Biogen Idec Inc.; Bristol-Myers Squibb Company; Eisai Inc.; Elan Pharmaceuticals, Inc.; Eli Lilly and Company; F. Hoffmann-La Roche Ltd and its affiliated company Genentech, Inc.; GE Healthcare; Innogenetics, N.V.; IXICO Ltd.; Janssen Alzheimer Immunotherapy Research & Development, LLC.; Johnson & Johnson Pharmaceutical Research & Development LLC.; Medpace, Inc.; Merck & Co., Inc.; Meso Scale Diagnostics, LLC.; NeuroRx Research; Novartis Pharmaceuticals Corporation; Pfizer Inc.; Piramal Imaging; Servier; Synarc Inc.; and Takeda Pharmaceutical Company. The Canadian Institute of Health Research is providing funds to support ADNI clinical sites in Canada. Private sector contributions are facilitated by the Foundation for the National Institutes of Health (www.fnih.org). The grantee organization is the Northern California Institute for Research and Education, and the study is coordinated by the Alzheimer’s Disease Cooperative Study at the University of California, San Diego. ADNI data are disseminated by the Laboratory for Neuro Imaging at the University of California, Los Angeles. This research was also supported by NIH grants P30 AG010129 and K01 AG030514.

References

- Ashburner J, Friston KJ. Unified segmentation. *Neuroimage*. 2005; 26(3):839–51. [PubMed: 15955494]
- Benitez BA, Cooper B, Pastor P, Jin SC, Lorenzo E, Cervantes S, Cruchaga C. *TREM2* is associated with the risk of Alzheimer’s disease in Spanish population. *Neurobiol Aging*. 2013; 34(6): 1711.e15–7. [PubMed: 23391427]
- Benitez BA, Cruchaga C. *TREM2* and neurodegenerative disease. *N Engl J Med*. 2013; 369(16):1567–8. [PubMed: 24131187]
- Bouchon A, Dietrich J, Colonna M. Cutting edge: inflammatory responses can be triggered by *TREM-1*, a novel receptor expressed on neutrophils and monocytes. *J Immunol*. 2000; 164(10): 4991–5. [PubMed: 10799849]
- Bush G, Luu P, Posner MI. Cognitive and emotional influences in anterior cingulate cortex. *Trends Cogn Sci*. 2000; 4(6):215–22. [PubMed: 10827444]

- Cash DM, Ridgway GR, Liang Y, Ryan NS, Kinnunen KM, Yeatman T, Malone IB, Benzinger TL, Jack CR Jr, Thompson PM, Ghetti BF, Saykin AJ, Masters CL, Ringman JM, Salloway SP, Schofield PR, Sperling RA, Cairns NJ, Marcus DS, Xiong C, Bateman RJ, Morris JC, Rossor MN, Ourselin S, Fox NC. The pattern of atrophy in familial Alzheimer disease: Volumetric MRI results from the DIAN study. *Neurology*. 2013; 18:18.
- Cavada C, Company T, Tejedor J, Cruz-Rizzolo RJ, Reinoso-Suarez F. The anatomical connections of the macaque monkey orbitofrontal cortex. A review. *Cereb Cortex*. 2000; 10(3):220–42. [PubMed: 10731218]
- Crane PK, Carle A, Gibbons LE, Insel P, Mackin RS, Gross A, Jones RN, Mukherjee S, Curtis SM, Harvey D, Weiner M, Mungas D. Development and assessment of a composite score for memory in the Alzheimer's Disease Neuroimaging Initiative (ADNI). *Brain Imaging Behav*. 2012; 6(4):502–16. [PubMed: 22782295]
- Cruchaga C, Fernandez-Seara MA, Seiyo-Martinez M, Samaranch L, Lorenzo E, Hinrichs A, Irigoyen J, Maestro C, Prieto E, Marti-Climent JM, Arbizu J, Pastor MA, Pastor P. Cortical atrophy and language network reorganization associated with a novel progranulin mutation. *Cereb Cortex*. 2009; 19(8):1751–60. [PubMed: 19020205]
- Cuadra MB, Cammoun L, Butz T, Cuisenaire O, Thiran JP. Comparison and validation of tissue modelization and statistical classification methods in T1-weighted MR brain images. *IEEE Trans Med Imaging*. 2005; 24(12):1548–65. [PubMed: 16350916]
- Folstein MF, Folstein SE, McHugh PR. "Mini-mental state". A practical method for grading the cognitive state of patients for the clinician. *J Psychiatr Res*. 1975; 12(3):189–98. [PubMed: 1202204]
- Forabosco P, Ramasamy A, Trabzuni D, Walker R, Smith C, Bras J, Levine AP, Hardy J, Pocock JM, Guerreiro R, Weale ME, Rytén M. Insights into TREM2 biology by network analysis of human brain gene expression data. *Neurobiol Aging*. 2013; 34(12):2699–714. [PubMed: 23855984]
- Gibbons LE, Carle AC, Mackin RS, Harvey D, Mukherjee S, Insel P, Curtis SM, Mungas D, Crane PK. A composite score for executive functioning, validated in Alzheimer's Disease Neuroimaging Initiative (ADNI) participants with baseline mild cognitive impairment. *Brain Imaging Behav*. 2012; 6(4):517–27. [PubMed: 22644789]
- Goni J, Cervantes S, Arrondo G, Lamet I, Pastor P, Pastor MA. Selective brain gray matter atrophy associated with APOE epsilon4 and MAPT H1 in subjects with mild cognitive impairment. *J Alzheimers Dis*. 2013; 33(4):1009–19. [PubMed: 23064258]
- Guerreiro R, Wojtas A, Bras J, Carrasquillo M, Rogaeva E, Majounie E, Cruchaga C, Sassi C, Kauwe JS, Younkin S, Hazrati L, Collinge J, Pocock J, Lashley T, Williams J, Lambert JC, Amouyel P, Goate A, Rademakers R, Morgan K, Powell J, St George-Hyslop P, Singleton A, Hardy J. TREM2 variants in Alzheimer's disease. *N Engl J Med*. 2013; 368(2):117–27. [PubMed: 23150934]
- Guerreiro RJ, Lohmann E, Bras JM, Gibbs JR, Rohrer JD, Gurunlian N, Dursun B, Bilgic B, Hanagasi H, Gurvit H, Emre M, Singleton A, Hardy J. Using exome sequencing to reveal mutations in TREM2 presenting as a frontotemporal dementia-like syndrome without bone involvement. *JAMA Neurol*. 2013; 70(1):78–84. [PubMed: 23318515]
- Hakola HP. Neuropsychiatric and genetic aspects of a new hereditary disease characterized by progressive dementia and lipomembranous polycystic osteodysplasia. *Acta Psychiatr Scand Suppl*. 1972; 232:1–173. [PubMed: 4509294]
- Hikosaka K, Watanabe M. Delay activity of orbital and lateral prefrontal neurons of the monkey varying with different rewards. *Cereb Cortex*. 2000; 10(3):263–71. [PubMed: 10731221]
- Ishii K, Sasaki H, Kono AK, Miyamoto N, Fukuda T, Mori E. Comparison of gray matter and metabolic reduction in mild Alzheimer's disease using FDG-PET and voxel-based morphometric MR studies. *Eur J Nucl Med Mol Imaging*. 2005; 32(8):959–63. [PubMed: 15800784]
- Jin SC, Pastor P, Cooper B, Cervantes S, Benitez BA, Razquin C, Goate A, Cruchaga C. Pooled-DNA sequencing identifies novel causative variants in PSEN1, GRN and MAPT in a clinical early-onset and familial Alzheimer's disease Ibero-American cohort. *Alzheimers Res Ther*. 2012; 4(4):34. [PubMed: 22906081]
- Jonsson T, Stefansson H, Steinberg S, Jonsdottir I, Jonsson PV, Snaedal J, Bjornsson S, Huttenlocher J, Levey AI, Lah JJ, Rujescu D, Hampel H, Giegling I, Andreassen OA, Engedal K, Ulstein I, Djurovic S, Ibrahim-Verbaas C, Hofman A, Ikram MA, van Duijn CM, Thorsteinsdottir U, Kong

- A, Stefansson K. Variant of TREM2 associated with the risk of Alzheimer's disease. *N Engl J Med.* 2013; 368(2):107–16. [PubMed: 23150908]
- Kahnt T, Chang LJ, Park SQ, Heinzle J, Haynes JD. Connectivity-based parcellation of the human orbitofrontal cortex. *J Neurosci.* 2012; 32(18):6240–50. [PubMed: 22553030]
- Klunemann HH, Ridha BH, Magy L, Wherrett JR, Hemelsoet DM, Keen RW, De Bleecker JL, Rossor MN, Marienhagen J, Klein HE, Peltonen L, Paloneva J. The genetic causes of basal ganglia calcification, dementia, and bone cysts: DAP12 and TREM2. *Neurology.* 2005; 64(9):1502–7. [PubMed: 15883308]
- Lanier LL, Bakker AB. The ITAM-bearing transmembrane adaptor DAP12 in lymphoid and myeloid cell function. *Immunol Today.* 2000; 21(12):611–4. [PubMed: 11114420]
- Lattante S, Le Ber I, Camuzat A, Dayan S, Godard C, Van Bortel I, De Septenville A, Ciura S, Brice A, Kabashi E. TREM2 mutations are rare in a French cohort of patients with frontotemporal dementia. *Neurobiol Aging.* 2013; 4(13)
- McKhann G, Drachman D, Folstein M, Katzman R, Price D, Stadlan EM. Clinical diagnosis of Alzheimer's disease: report of the NINCDS-ADRDA Work Group under the auspices of Department of Health and Human Services Task Force on Alzheimer's Disease. *Neurology.* 1984; 34(7):939–44. [PubMed: 6610841]
- Melchior B, Garcia AE, Hsiung BK, Lo KM, Doose JM, Thrash JC, Stalder AK, Staufenbiel M, Neumann H, Carson MJ. Dual induction of TREM2 and tolerance-related transcript, Tmem176b, in amyloid transgenic mice: implications for vaccine-based therapies for Alzheimer's disease. *ASN Neuro.* 2010; 2(3)
- Mittelbronn M, Dietz K, Schluesener HJ, Meyermann R. Local distribution of microglia in the normal adult human central nervous system differs by up to one order of magnitude. *Acta Neuropathol.* 2001; 101(3):249–55. [PubMed: 11307625]
- Mohs RC, Knopman D, Petersen RC, Ferris SH, Ernesto C, Grundman M, Sano M, Bieliauskas L, Geldmacher D, Clark C, Thal LJ. Development of cognitive instruments for use in clinical trials of antidementia drugs: additions to the Alzheimer's Disease Assessment Scale that broaden its scope. The Alzheimer's Disease Cooperative Study. *Alzheimer Dis Assoc Disord.* 1997; 11(Suppl 2):S13–21. [PubMed: 9236948]
- Montalbetti L, Ratti MT, Greco B, Aprile C, Moglia A, Soragna D. Neuropsychological tests and functional nuclear neuroimaging provide evidence of subclinical impairment in Nasu-Hakola disease heterozygotes. *Funct Neurol.* 2005; 20(2):71–5. [PubMed: 15966270]
- Morris JC. The Clinical Dementia Rating (CDR): current version and scoring rules. *Neurology.* 1993; 43(11):2412–4. [PubMed: 8232972]
- Ongur D, Ferry AT, Price JL. Architectonic subdivision of the human orbital and medial prefrontal cortex. *J Comp Neurol.* 2003; 460(3):425–49. [PubMed: 12692859]
- Ongur D, Price JL. The organization of networks within the orbital and medial prefrontal cortex of rats, monkeys and humans. *Cereb Cortex.* 2000; 10(3):206–19. [PubMed: 10731217]
- Paloneva J, Manninen T, Christman G, Hovanes K, Mandelin J, Adolfsson R, Bianchin M, Bird T, Miranda R, Salmaggi A, Tranebjaerg L, Kontinen Y, Peltonen L. Mutations in two genes encoding different subunits of a receptor signaling complex result in an identical disease phenotype. *Am J Hum Genet.* 2002; 71(3):656–62. [PubMed: 12080485]
- Parkin AJ, Java RI. Deterioration of frontal lobe function in normal aging: influences of fluid intelligence versus perceptual speed. *Neuropsychology.* 1999; 13(4):539–45. [PubMed: 10527062]
- Patterson N, Price AL, Reich D. Population structure and eigenanalysis. *PLoS Genet.* 2006; 2(12):e190. [PubMed: 17194218]
- Rajagopalan P, Hibar DP, Thompson PM. TREM2 and neurodegenerative disease. *N Engl J Med.* 2013; 369(16):1565–7. [PubMed: 24131186]
- Rayaprolu S, Mullen B, Baker M, Lynch T, Finger E, Seeley WW, Hatanpaa KJ, Lomen-Hoerth C, Kertesz A, Bigio EH, Lippa C, Josephs KA, Knopman DS, White CL 3rd, Caselli R, Mackenzie IR, Miller BL, Boczarska-Jedynak M, Opala G, Krygowska-Wajs A, Barcikowska M, Younkin SG, Petersen RC, Ertekin-Taner N, Uitti RJ, Meschia JF, Boylan KB, Boeve BF, Graff-Radford NR, Wszolek ZK, Dickson DW, Rademakers R, Ross OA. TREM2 in neurodegeneration:

- evidence for association of the p.R47H variant with frontotemporal dementia and Parkinson's disease. *Mol Neurodegener.* 2013; 8:19. 10–9. [PubMed: 23800361]
- Reitz C, Mayeux R. TREM2 and neurodegenerative disease. *N Engl J Med.* 2013; 369(16):1564–5. [PubMed: 24131184]
- Ruiz A, Dols-Icardo O, Bullido MJ, Pastor P, Rodriguez-Rodriguez E, Lopez de Munain A, de Pancorbo MM, Perez-Tur J, Alvarez V, Antonell A, Lopez-Arrieta J, Hernandez I, Tarraga L, Boada M, Lleo A, Blesa R, Frank-Garcia A, Sastre I, Razquin C, Ortega-Cubero S, Lorenzo E, Sanchez-Juan P, Combarros O, Moreno F, Gorostidi A, Elcoroaristizabal X, Baquero M, Coto E, Sanchez-Valle R, Clarimon J. Assessing the role of the TREM2 p.R47H variant as a risk factor for Alzheimer's disease and frontotemporal dementia. *Neurobiol Aging.* 2014; 35(2):444.e1–4. [PubMed: 24041969]
- Ryan NS, Keihaninejad S, Shakespeare TJ, Lehmann M, Crutch SJ, Malone IB, Thornton JS, Mancini L, Hyare H, Yousry T, Ridgway GR, Zhang H, Modat M, Alexander DC, Rossor MN, Ourselin S, Fox NC. Magnetic resonance imaging evidence for presymptomatic change in thalamus and caudate in familial Alzheimer's disease. *Brain.* 2013; 136(Pt 5):1399–414. [PubMed: 23539189]
- Scheltens P, Barkhof F, Leys D, Pruvo JP, Nauta JJ, Vermersch P, Steinling M, Valk J. A semiquantitative rating scale for the assessment of signal hyperintensities on magnetic resonance imaging. *J Neurol Sci.* 1993; 114(1):7–12. [PubMed: 8433101]
- Shaw LM, Vanderstichele H, Knapik-Czajka M, Clark CM, Aisen PS, Petersen RC, Blennow K, Soares H, Simon A, Lewczuk P, Dean R, Siemers E, Potter W, Lee VM, Trojanowski JQ. Cerebrospinal fluid biomarker signature in Alzheimer's disease neuroimaging initiative subjects. *Ann Neurol.* 2009; 65(4):403–13. [PubMed: 19296504]
- Takahashi K, Rochford CD, Neumann H. Clearance of apoptotic neurons without inflammation by microglial triggering receptor expressed on myeloid cells-2. *J Exp Med.* 2005; 201(4):647–57. [PubMed: 15728241]
- Tombaugh TN. Trail Making Test A and B: normative data stratified by age and education. *Arch Clin Neuropsychol.* 2004; 19(2):203–14. [PubMed: 15010086]
- Williams BW, Mack W, Henderson VW. Boston Naming Test in Alzheimer's disease. *Neuropsychologia.* 1989; 27(8):1073–9. [PubMed: 2797414]
- Yesavage JA, Brink TL, Rose TL, Lum O, Huang V, Adey M, Leirer VO. Development and validation of a geriatric depression screening scale: a preliminary report. *J Psychiatr Res.* 1982; 17(1):37–49. [PubMed: 7183759]

A detailed cross-sectional clinical and neuroimaging study of AD/MCI *TREM2* p.R47H carriers compared with noncarriers.

TREM2 p.R47H variant was associated with certain clinical and neuroimaging AD features.

Specifically, a high frequency of behavioural symptoms were found among *TREM2* p.R47H carriers.

In addition to the typical AD grey matter loss, authors found a preferential fronto-basal gray matter cortical loss among *TREM2* p.R47H mutation carriers.

These results suggest that frontobasal and temporal regions could be more susceptible to the deleterious biological effects of *TREM2* p.R47H.

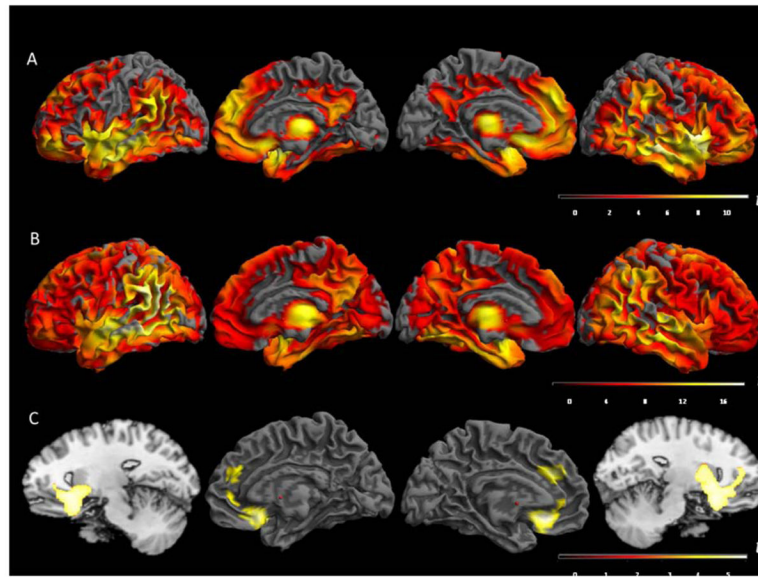


Figure 1.

Joint Analysis displaying gray matter loss on the rendered surface of the brain, in the following contrasts: A. Contrast AD/MCI *TREM2* p.R47H carriers vs. cognitively intact *TREM2* p.R47H noncarriers; B. Contrast AD/MCI no-*TREM2* mutation carriers vs. cognitively intact *TREM2* p.R47H noncarriers and C. Contrast AD/MCI *TREM2* p.R47H carriers vs. AD/MCI *TREM2* p.R47H noncarriers. The sagittal images had been added to display the basal ganglia gray matter loss. T-test scores scale. Threshold $p < 0.05$, FWE cluster-wise $p < 0.001$. AD: Alzheimer disease. MCI: mild cognitive impairment.

Table 1

Comparison of demographic and clinical data between *TREM2* p.R47H carriers and noncarriers from both sets.

	AD/MCI <i>TREM2</i> p.R47H carriers	AD/MCI <i>TREM2</i> p.R47H noncarriers	Healthy p.R47H <i>TREM2</i> noncarriers	corrected <i>p</i> values
n	MCI	7	20	
	AD	11	55	
	<i>Total</i>	18	75	75
Gender (% female)	MCI	28.6	23.5	
	AD	54.5	60.3	
	<i>Total</i>	44.4	52	49.3
Age at evaluation, yr	MCI	78.5 ± 7.1 (70.4–90.9)	78.7 ± 5.1 (72.6–90.6)	
	AD	71.7 ± 10.6 (57.5–84)	71.0 ± 7.9 (52.1–90.9)	
	<i>Total</i>	74.3 ± 9.8 (57.5–90.9)	72.8 ± 8 (52.1–90.9)	70.6 ± 8.8 (55–89.8)
Age at onset, yr	MCI	77.2 ± 6.5 (69.9–89.1)	74.9 ± 4.5 (72.1–89.4)	
	AD	67.9 ± 9.9 (55.6–80)	68.2 ± 8.1 (48.5–89.2)	
	<i>Total</i>	71.6 ± 9.7 (55.6–89.1)	70.3 ± 8.3 (48.5–89.4)	70.3 ± 8.3 (48.5–89.4)
Positive family history* (%)	MCI	71.4	47.1	
	AD	50	53.1	
	<i>Total</i>	58.8	51.5	48
MMSE	MCI	22.9 ± 6.4 (11–29)	26.5 ± 3.9 (15–30)	
	AD	14.6 ± 8.2 (4–26)	19.6 ± 4.8 (8–29)	
	<i>Total</i>	18 ± 8.4 (4–29)	21.16 ± 5.43 (8–30)	21.16 ± 5.43 (8–30)

	AD/MCI <i>TREM2</i> p.R47H carriers	AD/MCI <i>TREM2</i> p.R47H noncarriers	Healthy p.R47H <i>TREM2</i> noncarriers	corrected <i>p</i> values
Scheltens scale	MCI	6.4 ± 3.8 (0–13)	11.3 ± 5.9 (0–24)	
	AD	8.7 ± 5.2 (5–21)	8.4 ± 6.4 (0–27)	
	Total	7.69 ± 4.64 (0–21)	9 ± 6.37 (0–27)	n.s.
APOE (%) (n MCI/n AD)				
23	0	1.33 (0/1)	65.27	<0.001#
24	0	1.33 (0/1)	1.38	
33	50 (2/7)	40 (10/20)	26.38	
34	38.88 (3/4)	42.66 (8/24)	5.55	
44	11.12 (2/0)	14.68 (2/9)	2.77	

Numerical data are presented as mean ± standard deviation (range). Categorical data are presented as percentage.

* 1st degree family history of dementia. n.s. nonsignificant statistical differences.

Distribution of APOE genotype frequencies was statistically different between cognitively impaired (both AD/MCI p.R47H carriers and noncarriers) and healthy subjects for all genotypes except for APOE 24 for which showed no statistically significant differences in frequency distribution.

+ Other neuropsychological tests did not showed any significant difference between both AD/MCI groups. The level of significance considered was 0.05.

All *p*-values were two sided. Bonferroni correction was applied for multiple comparisons.

Table 2

Comparison of clinical data between Spanish AD *TREM2* p.R47H carriers and noncarriers.

	AD p.R47H <i>TREM2</i> carriers	AD p.R47H <i>TREM2</i> noncarriers	corrected <i>p</i> values
n	9	48	
First symptom			
Forgetfulness	(7/9) 77.8	(44/48) 91.7	n.s.
Depression	(2/9) 22.2	(0/48) 0	n.s.
Other [#]	(0/9) 0	(4/48)	n.s.
Early signs/symptoms [*]			
Psychiatric symptoms	(9/9) 100	(22/48) 45.8	0.039
Personality changes	(8/9) 88.9	(18/48) 37.5	n.s.
Spatial disorientation	(8/9) 88.9	(16/48) 33.3	0.01
Memory impairment	(9/9) 100	(47/48) 97.9	n.s.
Aphasia	(9/9) 100	(37/48) 77.1	n.s.
Apraxia	(9/9) 100	(15/48) 48	<0.0001
Agnosia	(3/9) 33.3	(12/48) 25	n.s.
Dysexecutive syndrome	(7/9) 71.4	(38/48) 79.2	n.s.
Primitive reflexes	(6/9) 57.1	(23/48) 41.7	n.s.
Parkinsonian signs	(6/9) 66.7	(7/48) 14.6	0.039

Data are presented as frequency and percentage and compared using the exact χ^2 -test. n.s. non significant statistical differences.

[#]This category included the following symptoms: nervousness, aphasia and spatial disorientation.

^{*} Early signs/symptoms were considered when they appeared during the first two years after disease onset.

Table 3

Conditional logistic regression model analyzing the relationship between neuropsychological variables and *TREM2* p.R47H status.

Cognitive domain	Neuropsychological test	Coefficient	Standard Error	Z Statistic	Uncorrected p value	Odds Ratio	95% CI
Daily living activities	<i>CDR</i> *	1.3780	1.1837	1.1641	0.2444	3.9669	0.3898–40.3685
	<i>MMSE</i> §	-0.1593	0.0620	-2.5706	0.0102 ⁺	0.8257	0.7552–0.9629
Psychiatric symptoms	<i>GDS 15</i> *	0.1125	0.1880	0.5980	0.5498	1.1190	0.7741–1.6177
	<i>GDS 30</i> [#]	0.0578	0.1077	0.5370	0.5913	1.0596	0.8579–1.3086
Executive functions	<i>ADNI_EF</i> *	-0.0614	0.4157	-0.1477	0.8826	0.9405	0.4164–2.1240
	<i>Semantic verbal fluency</i> §	0.0000	0.1250	0.0000	1.0000	1.0000	0.7827–1.2776
	<i>Trail making A</i> §	-0.0107	0.0075	-1.4304	0.1526	0.9893	0.9749–1.0040
	<i>Trail making B</i> §	-0.0055	0.0051	-1.0899	0.2758	0.9945	0.9846–1.0044
Memory	<i>ADAS word list</i>	0.0025	0.1718	0.0143	0.9886	1.0025	0.7159–1.4037
	<i>- 3rd trial</i> §	-0.0245	0.1725	-0.1420	0.8871	0.9758	0.6958–1.3684
	<i>- differed</i> §	-0.2230	0.4926	-0.4528	0.6507	0.8001	0.3046–2.1012
Language	<i>Boston (30 items)</i> *	0.1001	0.1272	0.7872	0.4312	1.1053	0.8614–1.4182
	<i>Boston (60 items)</i> [#]	-0.1280	0.1145	-1.1182	0.2635	0.8799	0.7030–1.1011

* ADNI1 set;

[#] Spanish set;

§ ADNI1 and Spanish set.

⁺ p-value=0.1326 after correcting for multiple comparisons.

Table 4

Joint analysis. Volumetric gray matter loss contrast between AD/MCI *TREM2* p.R47H carriers versus AD/MCI *TREM2* noncarriers.

Area	Side	BA	K	T	X	Y	Z
Frontal							
<i>Rectal Gyrus Orbitofrontal Cortex</i>	R	11	7089	4.50	20	18	-14
	L			4.49	-9	26	-12
	R			4.28	12	29	-15
<i>Superior frontal Gyrus</i>	L	6		4.09	-6	38	28
<i>Anterior Cingulate Cortex</i>	R	32		3.81	14	42	22
	R			3.42	15	48	10
	L			3.25	-6	41	1
Basal Ganglia							
<i>Putamen</i>	R			3.74	32	9	-5
	L			3.43	-10	7	-3
<i>Caudate</i>	R		7089	3.28	13	9	-5
	L			3.43	-10	9	-3
<i>Accumbens</i>	R			3.15	12	8	-8
	L			3.59	-10	8	-8

Statistically significant gray matter loss. Side: laterality; BA: Brodmann Areas; K: number of voxels per cluster, $p < 0.05$ FWE cluster-wise corrected $p = 0.001$; T-test score; x,y,z: MNI coordinates.